HOKKAIDO UNIVERSITY

Title	Facile Tuning of Hydrogel Properties by Manipulating Cationic-Aromatic Monomer Sequences
Author(s)	Fan, Hailong; Cai, Yirong; Gong, Jian Ping
Citation	SCIENCE CHINA Chemistry, 64(9), 1560-1568 https://doi.org/10.1007/s11426-021-1010-3
Issue Date	2021-08-12
Doc URL	https://hdl.handle.net/2115/86544
Rights	The original publication is available at www.scichina.com and www.springerlink.com
Type	journal article
File Information	manuscript.pdf,

Hokkaido University Collection of Scholarly and Academic Papers : HUSCAP

Facile Tuning of Hydrogel Properties by Manipulating Cationic-Aromatic Monomer Sequences

Hailong Fan,[1] Yirong Cai,[2] and Jian Ping Gong[1,3,4*]

[1]Institute for Chemical Reaction Design and Discovery (WPI-ICReDD), Hokkaido University, Sapporo 001-0021, Japan

[2]Graduate School of Life Science, Hokkaido University, Sapporo 001-0021, Japan

[3]Faculty of Advanced Life Science, Hokkaido University, Sapporo 001-0021, Japan

[4]Global Station for Soft Matter GI-CoRE, Hokkaido University, Sapporo 001-0021, Japan

*Correspondence to: gong@sci.hokudai.ac.jp

Abstract:

Copolymer hydrogels formed from cationic and aromatic monomers with identical monomer compositions but different average sequences were synthesized by free-radical copolymerization in various solvents. We found that hydrogels with one-component-rich segments are mechanically stronger than those with adjacent-rich monomer sequences in water, while hydrogels with a rich cation-π adjacent sequence showed excellent mechanical strength and underwater adhesion in saltwater (0.7 M NaCl). The molecular mechanisms for these behaviors are discussed in terms of polymer structures. This work reveals the importance of monomeric sequences in determining hydrogel properties and provides a facile approach to develop hydrogels with different properties but the same monomer composition.

Introduction

The excellent functionalities of biological systems are essentially due to the genetically pre-determined first-order structures of biopolymers, which govern the specific high-order structures of biological tissues to perform the necessary functions.[1-4] This indicates that for developing synthetic functional hydrogels, it is essential to not only explore the monomer species and compositions but also control their sequences in the constituent polymers. Although several advanced strategies have been developed to synthesize polymers with well-defined monomer sequences, most are only applicable to hydrophobic monomers, and it is difficult to apply them directly to hydrogel fabrication.[5-8] Moreover, these state-of-the-art synthetic methods usually have low yields, which is another factor that limits their application to material fabrication.[9] Consequently, studies on the influence of the monomer sequence on hydrogel properties are relatively limited and focus mainly on the thermoresponsive properties and swelling behaviors.[10, 11]

Free-radical polymerization is used frequently for the facile fabrication of hydrogel materials from monomers, mainly because of the ease of production and commercial availability of monomers with diverse functionalities. The copolymerization of monomers further enables the development of polymer materials with various chemical structures. Therefore, exploring the possibility of using free-radical polymerization to control the monomer sequence and sequence distribution in hydrogels is highly valuable and might provide a facile approach to develop hydrogels with different properties from the same composition of monomers. Moreover, identifying the role of the monomer sequences will also provide insights into understanding the mechanism behind the properties of the materials.

In copolymerization, the statistical distribution of the monomer sequences is governed by the reactivity ratio of monomers (r) and the monomer composition fractions f.[12] The reactivity ratio of monomers is influenced by several factors, such as the chemical structure, solvent, reaction temperature, and monomer concentration.[12] Due to the statistical reaction process, the monomer sequence in the copolymer changes with the monomer conversion during the polymerization, except that the infeed monomer fraction (f) is at the azeotropic point.[12] Moreover, to form network structures of hydrogels, chemical crosslinkers (usually di- or tri-functional monomers) are added for imparting crosslinking to polymer architectures. The addition of chemical crosslinkers to the polymers is also statistical and changes with monomer conversion.[13, 14] As a result, the properties of network materials and hydrogels are determined by the average monomer sequence and network architectures. Therefore, it is not possible to control the monomer sequences precisely using free-radical polymerization because of their statistical nature. Nevertheless, it is expected that the hydrogel properties can be tuned by changing the statistical distribution of the monomer sequence through control of the reactivity ratio of monomers (r) at a fixed monomer composition fraction (f).

In our previous work, it was found that the free-radical copolymerization behavior of cationic and aromatic monomer pairs (equimolar ratio) in their co-solvent DMSO depends on the total monomer concentration (C_M).[15] At low C_M (< 1.0 M), copolymers with a one-component-rich segment sequence are formed, whereas at high C_M (≥ 1.0 M), copolymers have cationic-aromatic adjacent-rich sequences. Accordingly, this method can be used to synthesize hydrogels with cationic-aromatic adjacent-rich sequences at a high C_M (Figure 1a). However, this method cannot be applied to synthesize hydrogels with a one-component-rich segment sequence

because hydrogel fabrication requires a high monomer concentration.

In this work, we intend to establish a facile method to synthesize hydrogels from the same pair of monomers but the different average sequences and to study the effect of the monomer sequence on the properties of bulk hydrogels. First, we discovered that dimethyl sulfate (DMS) can be a cosolvent of cationic monomers and aromatic monomers, and in DMS, the reactivity ratio (r) of both monomers is much larger than one; that is, both monomers prefer to react with themselves. Thus, hydrogels can be synthesized in DMS for a one-component-rich sequence (Figure 1a). Based on this, we fabricated hydrogels in DMSO and DMS solvents from two different cationic-aromatic monomer pairs and studied the effect of monomer sequences on their network structures as well as various properties, including swelling degrees, rheological properties, mechanical strength, and adhesiveness in water and saline solutions.

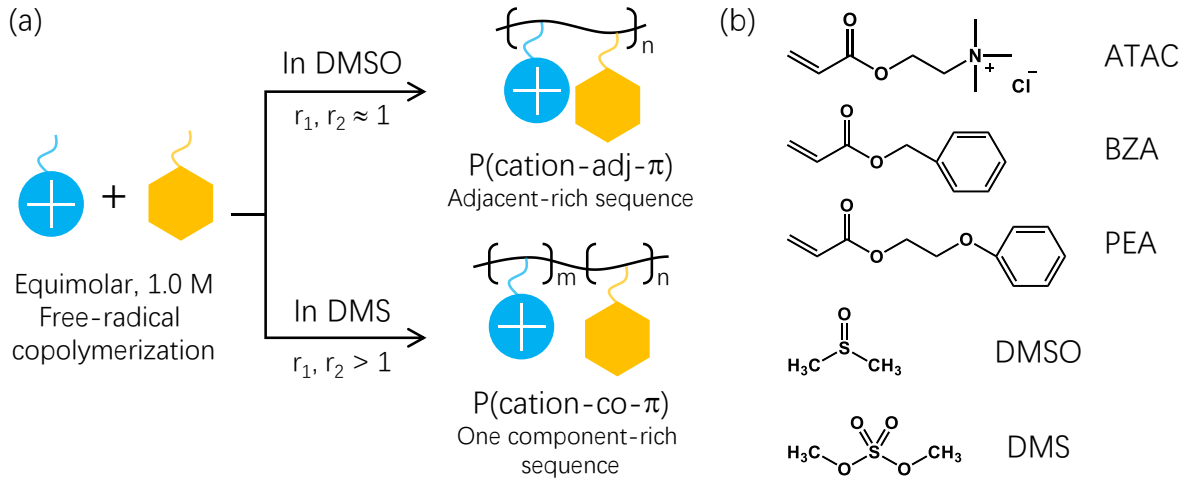

Figure 1. (a) Free-radical polymerization to synthesize copolymers with different cation-π sequences by using various solvents. (b) Chemical structures of cationic monomer, aromatic monomers, and solvents used in this work.

Results and Discussion

Copolymerization kinetics of monomer pairs.

We studied the copolymerization kinetics of cationic and aromatic monomer pairs (equimolar) in different solvents. In the DMSO solution, the conversion rates of the cationic and aromatic monomer pairs matched perfectly for both the ATAC-BZA pair (Figure 2a) and the ATAC-PEA pair (Figure 2b). In contrast, the conversion rates of the monomers differed significantly in the DMS solution; the cationic monomer was consumed faster than the aromatic monomer for both pairs (Figure 2c and 2d).

To understand the monomer sequence of the copolymers, we studied the reactivity ratio (r) of the monomers. The reactivity ratio for each propagating chain end is defined as the ratio of the rate constant for the addition of a monomer of the species already at the chain end to the rate constant for the addition of another monomer.[12] In general, r can be determined from the relationship between the monomer composition in the feed (f) and in the copolymer (F) formed at the initial stage of the reaction (total monomer conversion <10%). Accordingly, we studied the F–f relationship of the ATAC monomer copolymerized in DMSO and DMS solvent for the ATAC-BZA pair (Figure 2e) and ATAC-PEA pair (Figure 2f). In DMSO, the matched reaction occurs ($F_{ATAC} \approx f_{ATAC}$). In the DMS solvent, F_{ATAC} was larger than f_{ATAC} during the initial conversions. The reactivity ratios of the monomers were calculated (Table 1) by applying the data for the Mayo-Lewis equation.[16] In DMSO, the reactivity ratios of both cationic and aromatic monomers are close to one, indicating that the monomers show no preference for each other during polymerization; in other words, they copolymerize in a nearly ideal random manner. In contrast, the reactivity ratios of both cationic monomers and aromatic monomers in the DMS

solvent are much larger than 1, indicating that both monomers prefer to react strongly with each other.

Based on the monomer reactivity ratio, the instantaneous number-average sequence length of monomer $\langle N_M \rangle$ in polymer chains at different conversion p values were calculated for the equimolar ratio f_{ATAC} =0.5 (Equations S5 and S6), and the results for ATAC- BZA and ATAC-PEA are shown in Figure 2g and 2h, respectively.[17, 18] For copolymers synthesized from DMSO solvent, the $\langle N_M \rangle$ values of both cationic and aromatic monomers are very small ($\langle N_M \rangle \approx 2$) and do not vary with the conversion p. Therefore, most monomers (~ 73%) are in the adjacent location (Equation S13). Hereinafter, the copolymers synthesized in DMSO are referred to as P(cation-adj-π) (adj is short for adjacent, π is short for aromatic monomer). For copolymers synthesized in the DMS solvent, the $\langle N_M \rangle$ of both cationic and aromatic monomers is highly dependent on the conversion point. At low conversions, the polymer contained cationic-rich segments. As the polymerization reaction continued, cationic monomers were consumed first, and subsequently, the aromatic monomers began to polymerize into long sequence segments until all monomers were consumed. As a result, the copolymers had large component-rich segments. Hereinafter, the copolymers synthesized in DMS are referred to as P(cation-co-π).

The NMR spectrum of the copolymers also revealed the different sequences of aromatic monomers in the polymer chains (Figure 3). For P(cation-adj-π), the phenyl proton signals show symmetric broadening around the peak of the phenyl protons of aromatic monomers, indicating the adjacently dispersed cationic and aromatic residues on the polymer chains.[15] However, the signal of phenyl protons in P(cation-co-π) has new broad peaks at the higher field (Figure 3, yellow background), which are similar to those of aromatic homopolymers, indicating that the

aromatic monomers are homopolymerized into long segments in polymer chains.

The difference in the sequence results in significantly different water solubilities of the copolymers, although they have the same chemical composition, both containing 50 mol% of the hydrophobic aromatic unit. P(cation-adj-π) is water-soluble because the strong electrostatic repulsion of cationic residues prevents the nearby hydrophobic aromatic residues from aggregating in water. P(cation-co-π) is water-insoluble because the large aromatic-rich segments form aggregates that counterbalance the electrostatic repulsion and precipitate in water.

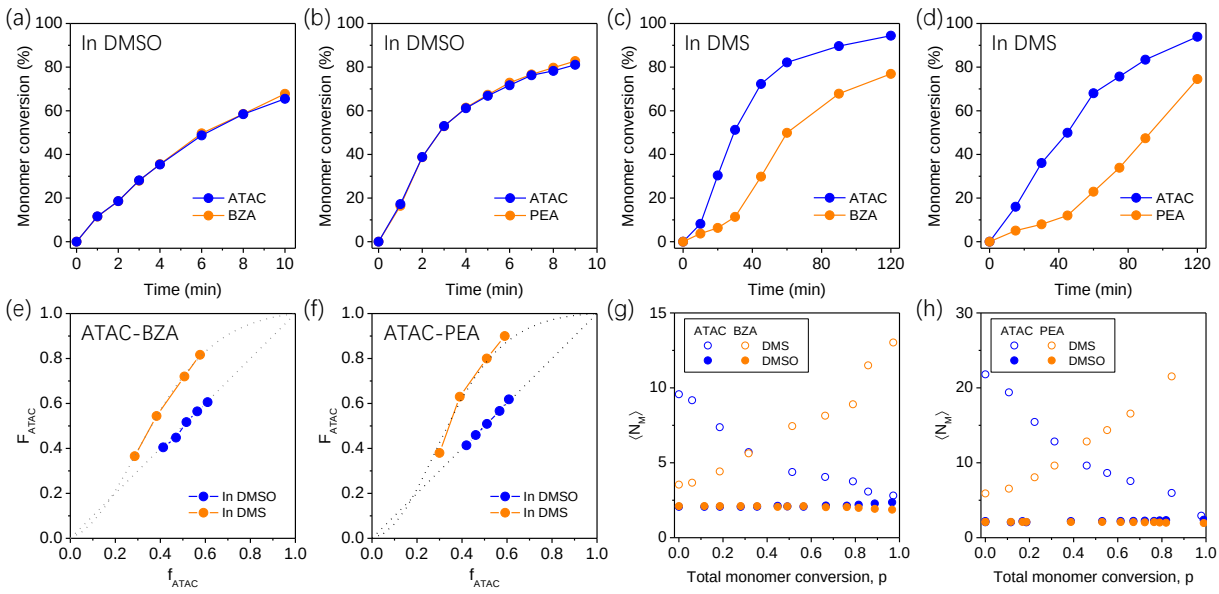

Figure 2. (a-d) Monomer conversion kinetics of cationic and aromatic monomers in the DMSO solvent (a, b) and DMS solvent (c, d) for two different pairs of cationic and aromatic monomers. The monomers were in equimolar ratio and the total monomer concentration was 1.0 M. (e, f) Relationship between the molar fraction of the cationic monomer in the feed (f_{ATAC}) and copolymer (F_{ATAC}) at a fixed total monomer concentration of 1.0 M for two different pairs of cationic and aromatic monomers. The conversion of monomers was less than 10%. The

experimental data (dots) were fitted by the Mayo-Lewis equation (grey dotted line). (g, h) Instantaneous number-average sequence length of monomer $\langle N_M \rangle$ versus the total monomer conversion *p* for the equimolar ratio of ATAC-BZA pair (g) and ATAC-PEA pair (h). The results in g, h are calculated using the monomer reactivity ratios shown in Table 1.

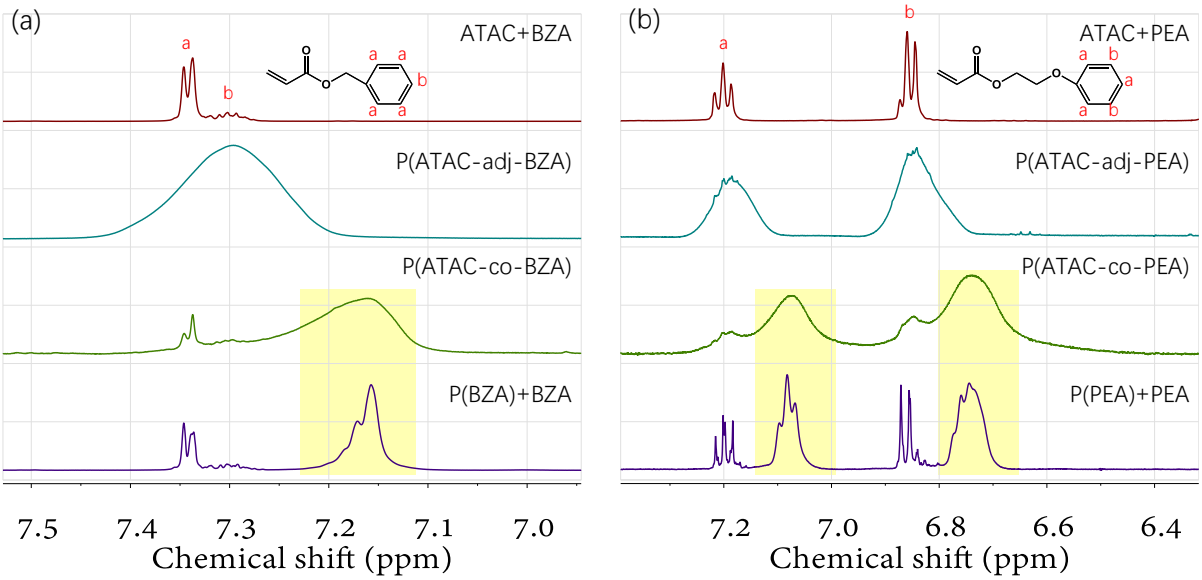

Figure 3. Partial (aromatic protons) ^{1}H NMR spectra of monomer mixtures, P(cation-adj-π), P(cation-co-π), and aromatic homopolymers containing a small number of aromatic monomers in DMSO-d_6 solution. (a) ATAC-BZA and (b) ATAC-PEA pairs. The yellow backgrounds highlight the proton peaks of long aromatic segments in polymer chains.

Table 1. Monomer reactivity ratios in DMSO and DMS solvents.

	ATAC-BZA pair		ATAC-PEA pair	
	r_{ATAC}	r_{BZA}	r_{ATAC}	r_{PEA}
In DMSO	1.07	1.11	1.16	1.15
In DMS	8.33	2.62	19.99	5.11

Swelling behavior of hydrogels.

Although the polymer sequences in this study were not precisely controlled, one-pot free-radical copolymerization allowed us to synthesize copolymers with different sequences on a large scale, which meets the requirements for material fabrication and studies. To evaluate the effect of the monomer sequence on the material properties, we further fabricated gels by the copolymerization of monomers at a high concentration (2.4 M) with a small amount of chemical crosslinker (0.1 mol% relative to the total monomer concentration) in DMSO and DMS. It should be noted that the influence of the distribution of chemical crosslinkers on polymer chains has not been considered because of their extremely low concentration.

In the synthesis of gels from the DMS system, during copolymerization, the mixture became turbid and solidified within minutes of UV irradiation, indicating the formation of a cationic-rich segment for which DMS is a poor solvent. Subsequently, the aromatic monomer polymerized into an aromatic-rich segment (Figure 2g and 2h). In contrast, the gels synthesized in the DMSO solvent were transparent, indicating that the P(cation-adj-π) gels had a homogeneous entangled polymer network structure. Hydrogels with the same monomer composition but different monomer sequences were obtained by replacing the organic solvents with water or salt water after synthesis.

The P(cation-adj-π) and P(cation-co-π) hydrogels, which had completely different monomer sequences and network structures, showed vastly different macroappearances in water and saltwater. The P(cation-adj-π) hydrogels were almost transparent, while the P(cation-co-π) hydrogels were opaque owing to the aggregation of hydrophobic aromatic-rich segments. Figure 4a shows photographs of the samples swollen in 0.7 M NaCl (ionic strength of seawater).

Because the polyelectrolyte chain conformation is significantly influenced by the salt

concentration, the hydrogels were swelled in water and NaCl solutions of different concentrations, and the relationship between the swelling ratio Q and the salt concentration Cs was studied (Figure 4b and 4c). The homo-polycationic P(ATAC) hydrogel has negligible shrinkage at low salt concentrations ($Cs < 10^{-2}$ M) but shrinks at high salt concentrations with a scaling relation $Q \sim Cs^{-1/2}$, which could be attributed to as the screening effect of the polyelectrolyte hydrogels in the salt solution. The high degree of swelling of polyelectrolyte hydrogels in water is dominated by the osmotic effect of mobile count-ions. When the salt concentration approached the polyion concentration, the ionic osmotic effect of the polyelectrolyte was suppressed, resulting in shrinkage of the hydrogel.[19, 20] P(cation-co-π) hydrogels have a much lower degree of swelling in pure water and salt solutions, which indicates that the hydrophobic aggregate structure has a strong ability to restrain the swelling of cationic-rich segments. Nevertheless, they exhibit a similar deswelling tendency at high salt concentrations, indicating the effect of charges on the swelling of the hydrogels. In contrast, although the P(cation-adj-π) hydrogels show slightly lower swelling than the P(ATAC) hydrogels comprising the pure polyelectrolyte, they shrink with increasing salt concentration in the entire range of salt concentrations studied ($10^{-4} \sim 0.7$ M), which is different from the behavior of pure polyelectrolyte hydrogels. The unique deswelling behavior of P(cation-adj-π) hydrogels at low salt concentrations suggests the interaction of salt ions with P(cation-adj-π). This interesting phenomenon is beyond the scope of this work and will be studied separately in future.

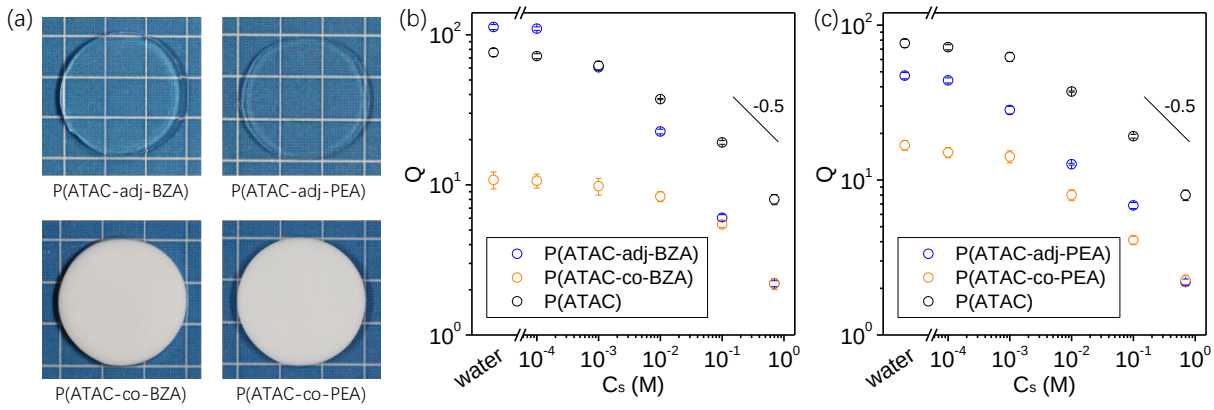

Figure 4. (a) Digital photos of P(cation-adj-π) and P(cation-co-π) hydrogels equilibrated in 0.7 M NaCl solution. (b, c) Volume swelling ratio (Q) of the hydrogels in relative to their as-prepared state vs. NaCl salt concentration C_s. For comparison, the data for homo-polyelectrolyte P(ATAC) are also shown. The error bars indicate the standard deviation (n = 3).

Dynamic rheological behavior of hydrogels.

To elucidate the structural differences between P(cation-adj-π) and P(cation-co-π) hydrogels, the dynamic rheological test was performed for the hydrogels equilibrated in water and 0.7 M NaCl. In water, the highly swollen P(cation-adj-π) hydrogels exhibit quasi-elastic behaviors, showing a weak frequency dependence of storage modulus G', which is much larger than the loss modulus G" (Figure 5a and 5b). Owing to the elastic behavior, we could not construct master curves for the P(cation-adj-π) hydrogels. In contrast, the P(cation-co-π) hydrogels exhibited distinct viscoelastic behaviors (Figure 5c and 5d), showing a clear tan δ peak around 10^4 rad s^{-1}, which is very similar to the rubbery-glassy relaxation peak for the homopolymers of poly(BZA) and poly(PEA).[21] This result suggests that the aromatic-rich polymer segments form relatively large hydrophobic aggregates and show the rubbery-glassy transition at high frequency. Moreover, the temperature dependence of the shift factor (a_T) of the P(cation-co-π)

hydrogels did not obey a single Arrhenius law, and the activation energy varied over a wide range from 90 to 300 kJ mol^{-1} (Figure S1), which indicates the wide distribution of hydrophobic associations.

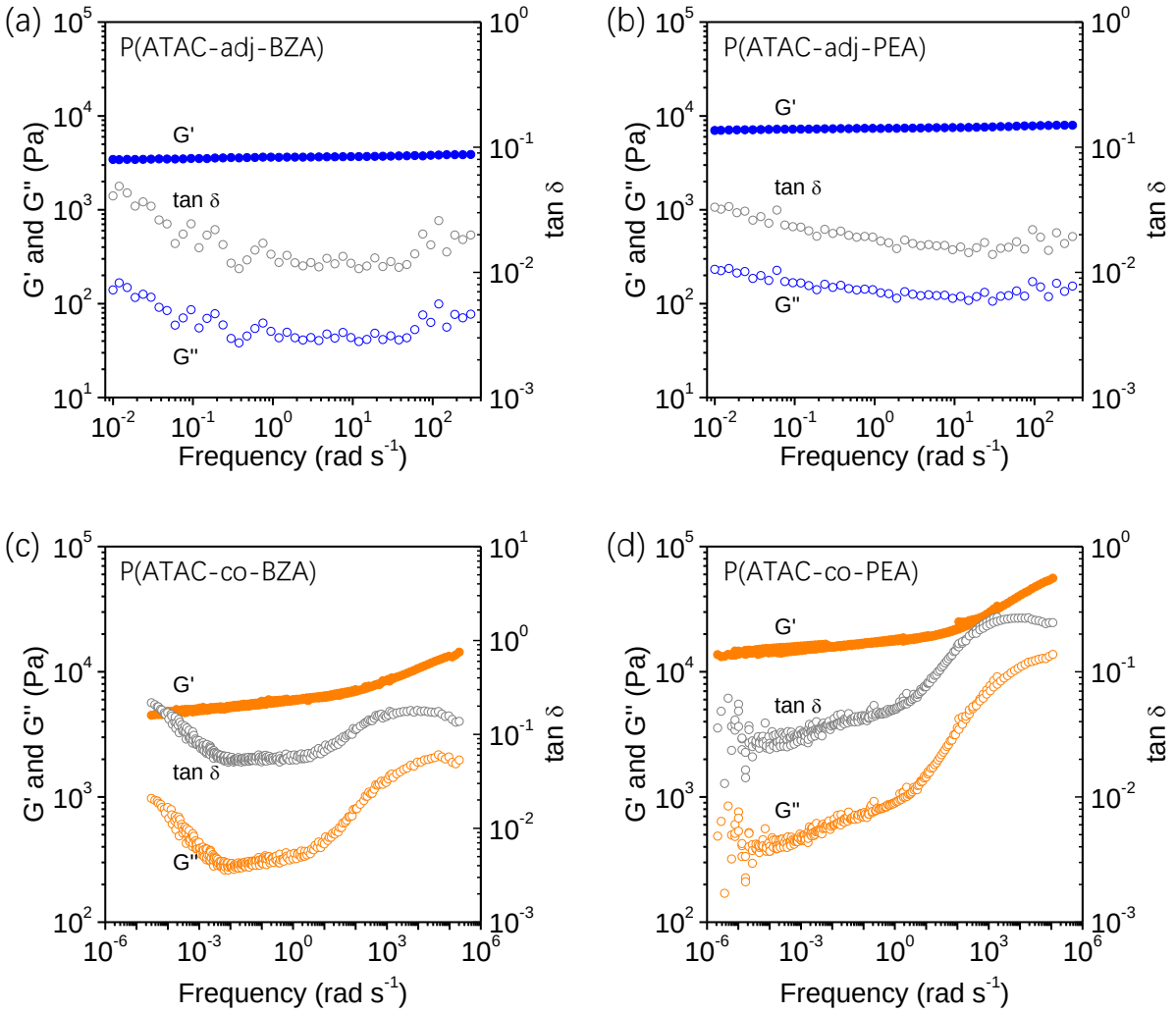

Figure 5. (a, b) Storage modulus G', loss modulus G", and loss factor (tanδ = G"/G') of P(cation-adj-π) hydrogels with angular frequency sweep. (c, d) Master curves of storage modulus G' and loss modulus G" of P(cation-co-π) hydrogels. All hydrogels were equilibrated in water.

In a 0.7 M NaCl solution, the hydrogels shrank considerably owing to the electrostatic screening effect of salt ions. Rheology measurements showed that both P(cation-adj-π) and P(cation-co-π) hydrogels exhibit viscoelastic properties, but their rheological curves are distinctly different, indicating the difference in the dynamic crosslinking mechanism of the network (Figure 6). The P(cation-adj-π) hydrogels show a clear tan δ peak in the vicinity of 10^0~10^1 rad s^{-1}, corresponding to the relaxation time of 0.1~1 s for both the ATAC-BZA and ATAC-PEA pairs. Furthermore, their shift factors denoted by a_T exhibit a single Arrhenius-type temperature dependence with an activation energy of approximately 80~100 kJ mol^{-1} (Figure S2). This relaxation time and activation energy are attributed to the aggregated cation-π associations in the network of the P(cation-adj-π) hydrogels. In contrast, the P(cation-co-π) hydrogels have two tan δ peaks at 10^{-1} ~ 10^{-2} rad s^{-1} and ~10^4 rad s^{-1}. The activation energy of P(cation-co-π) hydrogels varied over a wide range of 90~300 kJ mol^{-1} (Figure S2). The high frequency peak (~10^4 rad s^{-1}) has the same position as the swelling in water and can be assigned to the rubbery-glassy transition of the aggregated aromatic-rich polymer segments as in water. The new broad tan δ peak in the vicinity of 10^{-1} ~ 10^{-2} rad s^{-1} (corresponding to a relaxation time of 10 ~ 100 s), which is absent for the gels equilibrated in water, could be assigned to the aggregated cation-π associations. The cation-π association peak of P(cation-co-π) has a longer relaxation time (10 ~ 100 s) than P(cation-adj-π) (0.1~1 s), which could be explained by the stabilization of the cation-π association in a hydrophobic environment.

In summary, the P(cation-adj-π) hydrogels have a highly swollen elastic network in water, but they form dynamic bonds composed of relatively weak aggregated cation-π interactions (activation energy 80 ~100 kJ mol^{-1}) with a short lifetime (0.1~1 s) in saltwater (0.7 M NaCl).

In contrast, P(cation-co-π) hydrogels contain dynamic bonds composed of aggregated hydrophobic and cation-π interactions with a wide range of strength (activation energy 90~300 kJ mol^{-1}) in both water and 0.7 M NaCl solution.

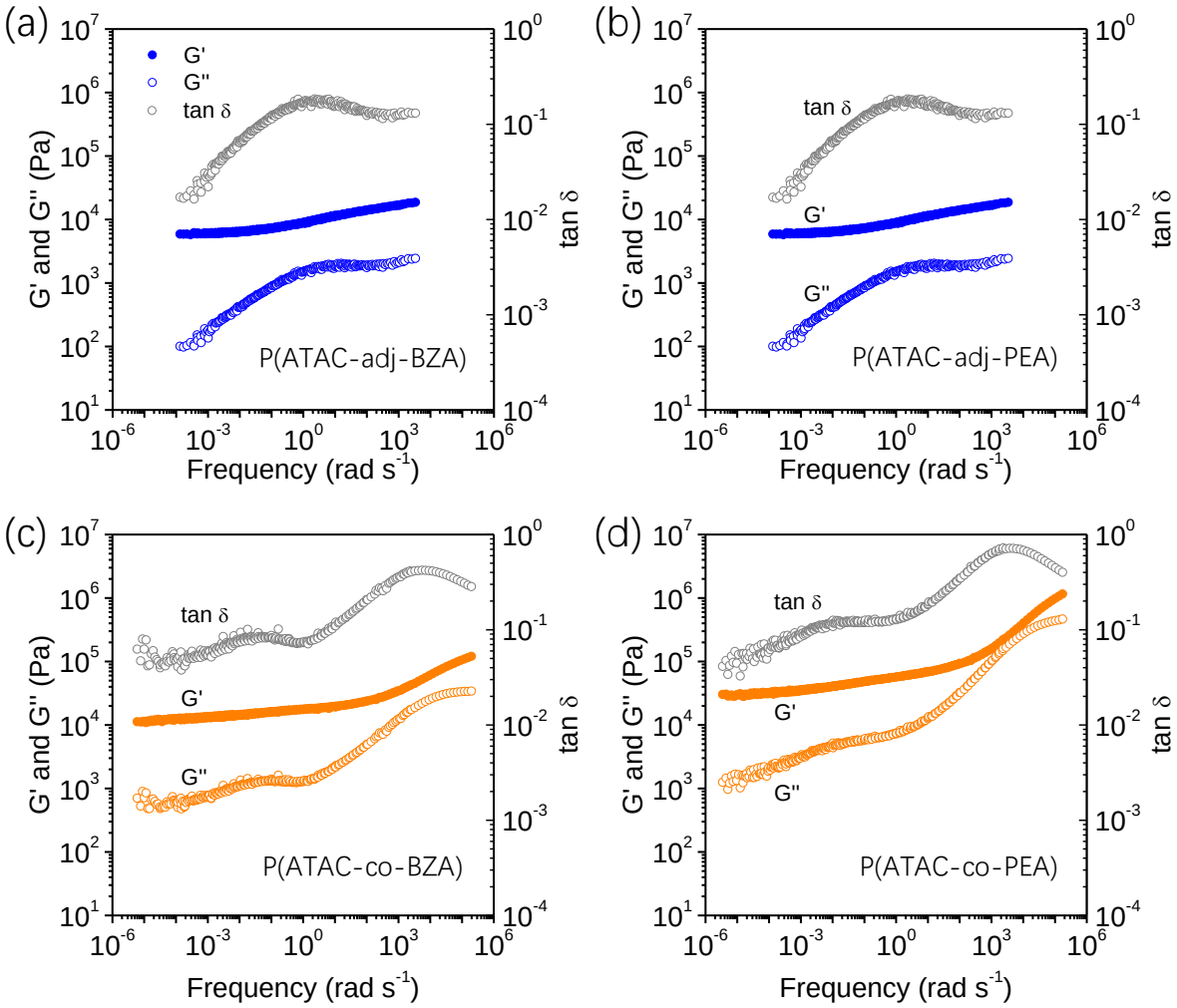

Figure 6. Master curves of storage modulus G', loss modulus G", and loss factor (tanδ = G"/G') of (a, b) P(cation-adj-π) hydrogels and (c, d) P(cation-co-π) hydrogels. All hydrogels were equilibrated in a 0.7 M NaCl solution.

Mechanical performance of hydrogels.

The differences in dynamic crosslinking influence the mechanical strength of hydrogels, as

determined by a uniaxial tensile test. In water, compared with the highly swollen P(cation-adj-π) hydrogels, which are mechanically weak and fragile, the P(cation-co-π) hydrogels are relatively strong and tough (Figure 7a and 7b). For example, the tensile strength of the P(ATAC-co-PEA) hydrogel was approximately 80 kPa with an elongation of 120% and an Young's modulus of approximately 0.05 MPa. Considering the differences in the swelling ratio of the hydrogels, we compared the tensile stress-strain curves of hydrogels normalized by the swelling ratio (Q) (Figure S3). It was found that the normalized mechanical strength of poly(cation-co-π) hydrogels was still considerably higher than that of the P(cation-adj-π) hydrogels with the same combination, which indicates that hydrophobic interactions have a considerable impact on the mechanical strength.

In a 0.7 M NaCl solution, the mechanical strength of hydrogels was significantly different from that in water. As shown in Figure 7c and 7d, at a strain rate of 0.14 s^{-1}, the P(cation-adj-π) hydrogels with short bond association times (0.1~1 s) are less strong but more stretchable (elongation > 700%) than the P(cation-co-π) hydrogels (elongation < 300%) with long bond association times (10~100 s) for both monomer pairs, although they have similar swelling ratios. Moreover, the largely formed cation-π associates in P(cation-adj-π) hydrogels impart them with a higher toughness than P(cation-co-π) hydrogels.

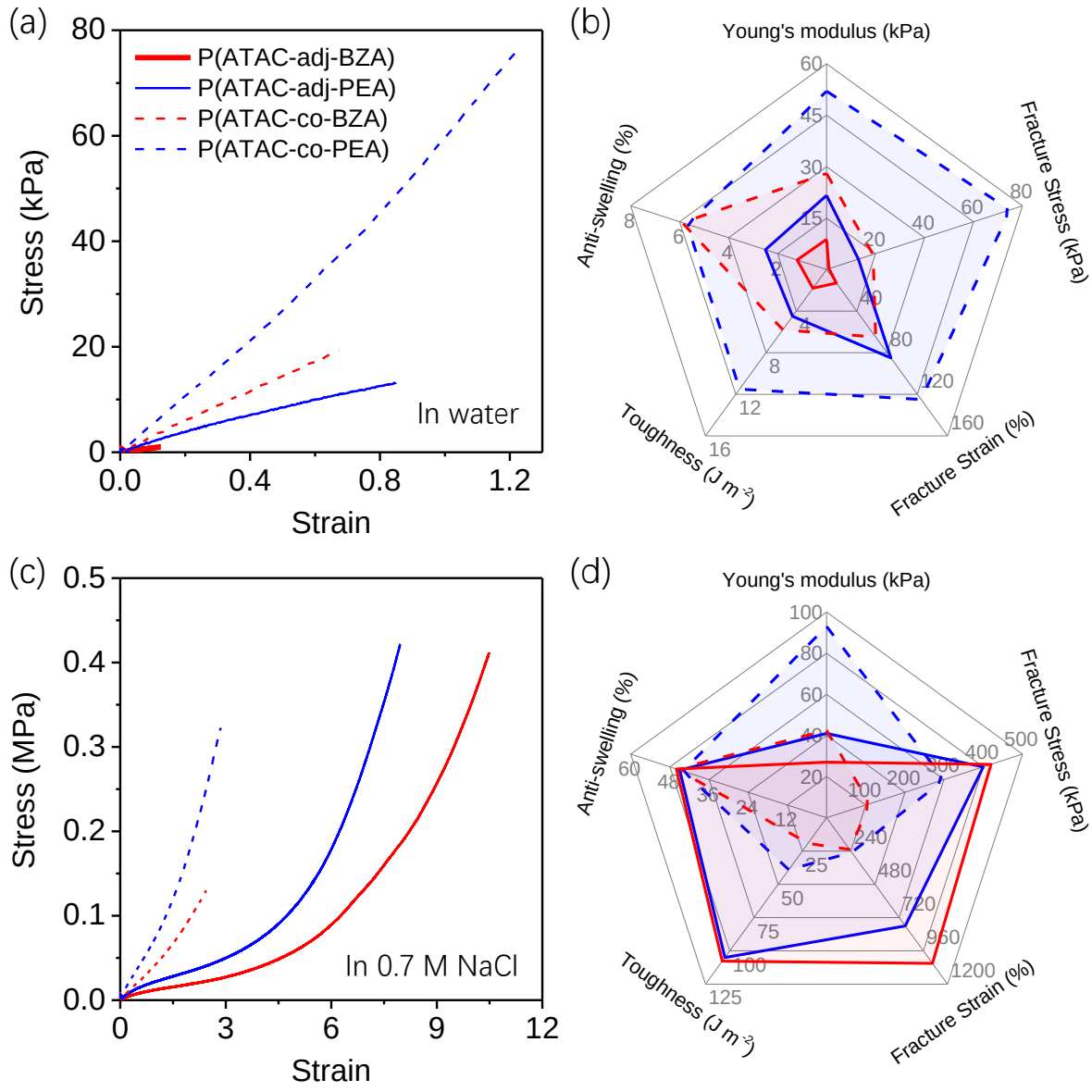

Figure 7. Mechanical strength of P(cation-adj-π) and P(cation-co-π) hydrogels equilibrated in (a, b) water and (c, d) 0.7 M NaCl solution. (a, c) Uniaxial tensile stress-strain curves of hydrogels. (b, d) Radial plots comparing Young's modulus, fracture stress, fracture strain, toughness, and anti-swelling ability of P(cation-adj-π) and P(cation-co-π) hydrogels. The anti-swelling ability is defined as 1/Q. All figures use the same legend as shown in Figure 7a.

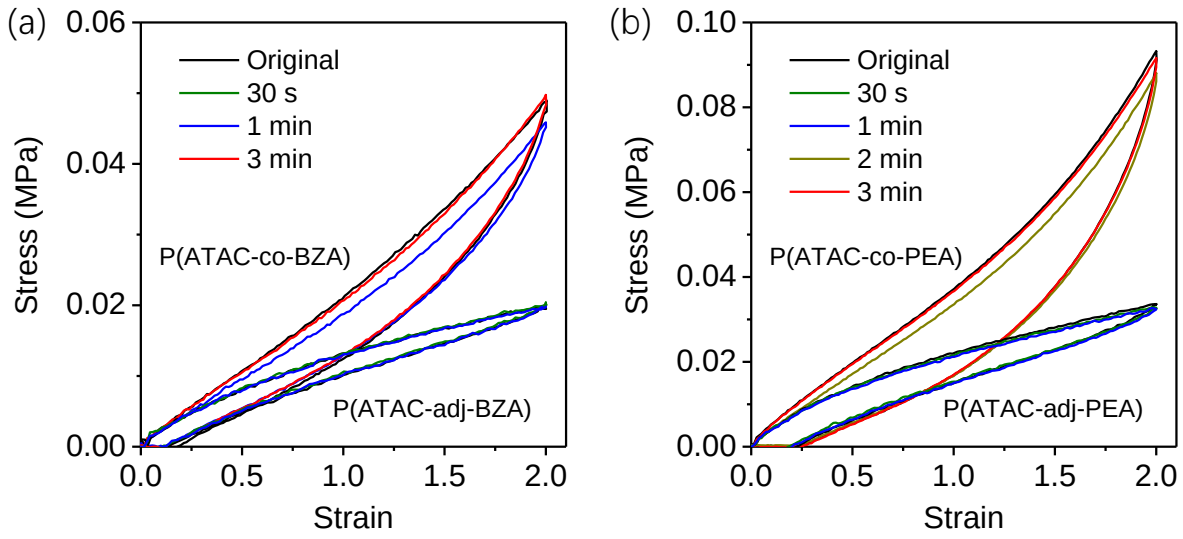

Figure 8. Cyclic loading-unloading curves of P(cation-adj-π) and P(cation-co-π) hydrogels equilibrated in 0.7 M NaCl solution. (a) Hydrogels fabricated from ATAC and BZA monomers. (b) Hydrogels fabricated from ATAC and PEA monomers. The waiting time between the sequential cyclic load is shown in the figures. The tensile tests were performed at a strain rate of 0.14 s^{-1}.

We further tested the energy dissipation and self-recovery abilities of hydrogels equilibrated in 0.7 M NaCl solution by the cyclic tensile test. Because the hydrogels have different physical associations originating from different monomer sequences, their energy dissipation ability and self-recovery speed also vary (Figure 8). At a strain of 200%, P(cation-adj-π) hydrogels recovered in 30 s, while P(cation-co-π) hydrogels required a longer time (3 min) to recover because of the stabilized cation-π interaction in a relatively hydrophobic environment.

Another difference between the hydrogels in terms of mechanical properties is their self-healing ability. Owing to the presence of a large number of dynamic bonds, P(cation-adj-π) hydrogels showed partial self-healing in saltwater. Figure S4 shows the tensile stress-strain

curves of the original and self-healed P(ATAC-adj-PEA) hydrogels. For the self-healed hydrogel, the sample was cut into half, and the fracture surfaces were kept in contact for 1 h under 0.7 M NaCl solution at room temperature. The results show that the cut hydrogels self-healed partially owing to the cation-π interactions at the interface. However, self-healing ability was not observed in the P(cation-co-π) hydrogels.

We also compared the mechanical properties of hydrogels with the same monomer sequences but different monomer types. The rheology results show that PEA-based P(cation-adj-π) hydrogels have a higher activation energy than the BZA-based ones. These results indicate that PEA can form stronger cation-π interactions with ATAC. We consider that PEA, which possesses a phenyl side group with a longer spacer, interacts more easily with the cationic groups than BZA, thereby enhancing their non-covalent interactions. Such differences in the physical interactions caused by the structure of the aromatic monomers also directly affect the mechanical strength of the hydrogels. Compared with the BZA-based hydrogels, the PEA-based hydrogels have not only higher mechanical strength but also better energy dissipation abilities (Figure S5).

Adhesion performance of hydrogels in saltwater.

The monomer sequence also had a strong impact on the underwater adhesion of the hydrogels (Figure 7). The tack test shows that P(cation-adj-π) hydrogels exhibit strong adhesion to negatively charged glass in saltwater (0.7 M NaCl) because the aromatic groups can enhance the electrostatic interactions of their adjacent cationic residues with the counter surfaces in high ionic mediums.[15, 22] In contrast, the P(cation-co-π) hydrogels, which lack adjacent cationic-aromatic sequences, exhibit weak adhesion on the glass substrate in saltwater. The P(cation-co-

π) hydrogels showed weaker adhesion than the P(cation-adj-π) hydrogels for the hydrophobic PMMA substrate as well. We consider that the large and rigid hydrophobic domains of P(cation-co-π) hydrogels cannot break the hydration layer at the interface to form strong hydrophobic interactions. This is consistent with the known fact that hydrophobic materials, without a specific water-breaking mechanism, do not adhere to each other in water.

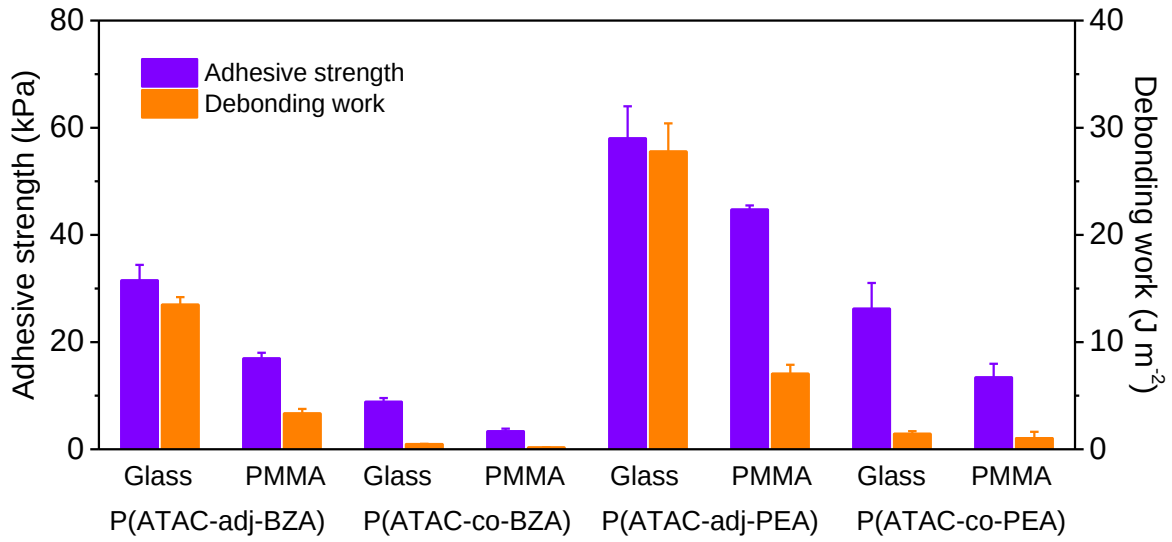

Figure 9. Adhesion performance of P(cation-adj-π) and P(cation-co-π) hydrogels to glass and PMMA substrates in 0.7 M NaCl solutions. The error bars indicate the standard deviation (n = 5).

Conclusion

Copolymers formed from cationic and aromatic monomers with identical monomer compositions but different average sequences were synthesized by free-radical copolymerization in various solvents. The calculated reactivity ratios indicate that the P(cation-adj-π) copolymer synthesized in DMSO shows ideal random copolymerization and has a rich

adjacent sequence of cationic-aromatic monomers. The monomers in DMS prefer to react with themselves during copolymerization, resulting in a one-component-rich sequence of P(cation-co-π). Consequently, the hydrogels fabricated from these two copolymers exhibited different properties. The P(cation-co-π) hydrogels have large hydrophobic aggregated structures; thus, they are opaque and exhibit strong anti-swelling ability, while P(cation-adj-π) hydrogels are almost transparent due to their higher water solubility. In water, P(cation-co-π) hydrogels are stronger than P(cation-adj-π) hydrogels because of their large hydrophobic associations. However, in saltwater (0.7 M NaCl), P(cation-adj-π) hydrogels have lower Young's modulus but are more stretchable and tougher than P(cation-co-π) hydrogels for the same strain rate. In addition, P(cation-adj-π) hydrogels in salt solution exhibit partial self-healing ability but the P(cation-co-π) hydrogels do not. The adhesion test shows that P(cation-adj-π) hydrogels have stronger adhesion in saltwater than P(cation-co-π) hydrogels on either negatively charged or hydrophobic substrates. This work provides a new approach for controlling the polymer sequence in hydrogels by tuning the reactivity ratios of the monomers. Moreover, this work indicates that the monomer sequence has a strong impact on the network structures and properties of related hydrogels, which has rarely been discussed in earlier studies.

AUTHOR INFORMATION

Corresponding Author

*E-mail gong@sci.hokudai.ac.jp (J.P.G.)

ORCID

Hailong Fan: 0000-0002-4900-1421

Jian Ping Gong: 0000-0003-2228-2750

Notes

The authors declare no competing financial interests.

ACKNOWLEDGMENT

This research was supported by JSPS KAKENHI Grant Numbers JP17H06144 and JP17H06376, and Institute for Chemical Reaction Design and Discovery (WPI-ICReDD) established by World Premier International Research Initiative (WPI), MEXT, Japan. The authors thank Mr. Yoshiyuki Saruwatari at Osaka Organic Chemistry Co., Ltd., Japan for providing monomers.

REFERENCES

1. Webber, M. J.; Appel, E. A.; Meijer, E. W.; Langer, R. Supramolecular biomaterials. *Nat. Mater.* **2016,** 15, 13-26.

2. Fan, H. L.; Gong, J. P. Fabrication of Bioinspired Hydrogels: Challenges and Opportunities. *Macromolecules* **2020,** 53, 2769-2782.

3. Lutz, J.-F.; Ouchi, M.; Liu, D. R.; Sawamoto, M. Sequence-Controlled Polymers. *Science* **2013,** 341, 1238149.

4. Lutz, J.-F.; Lehn, J.-M.; Meijer, E. W.; Matyjaszewski, K. From precision polymers to complex materials and systems. *Nat. Rev. Mater.* **2016,** 1, 16024.

5. Martens, S.; Holloway, J. O.; Du Prez, F. E. Click and Click-Inspired Chemistry for the Design of Sequence-Controlled Polymers. *Macromol. Rapid Commun.* **2017,** 38, 1700469.

6. Ouchi, M.; Sawamoto, M. Sequence-controlled polymers via reversible-deactivation radical polymerization. *Polym. J.* **2017,** 50, 83.

7. Pasini, D.; Takeuchi, D. Cyclopolymerizations: Synthetic Tools for the Precision Synthesis of Macromolecular Architectures. *Chem. Rev.* **2018,** 118, 8983-9057.

8. Meier, M. A. R.; Barner-Kowollik, C. A New Class of Materials: Sequence-Defined Macromolecules and Their Emerging Applications. *Adv. Mater.* **2019,** 31, 1806027.

9. Solleder, S. C.; Schneider, R. V.; Wetzel, K. S.; Boukis, A. C.; Meier, M. A. R. Recent Progress in the Design of Monodisperse, Sequence-Defined Macromolecules. *Macromol. Rapid Commun.* **2017,** 38, 1600711.

10. Ida, S.; Kawahara, T.; Kawabata, H.; Ishikawa, T.; Hirokawa, Y. Effect of Monomer Sequence along Network Chains on Thermoresponsive Properties of Polymer Gels. *Gels* **2018,** 4, 22.

11. Kimura, M.; Fukumoto, K.; Watanabe, J.; Takai, M.; Ishihara, K. Spontaneously Forming Hydrogel From Water-soluble Random- and Block-type Phospholipid Polymers. *Biomaterials* **2005,** 26, 6853-6862.
12. Odian, G. Principles of Polymerization, 4th ed. *Wiley-Interscience: Hoboken, NJ* **2004**.
13. Gao, H.; Miasnikova, A.; Matyjaszewski, K. Effect of Cross-Linker Reactivity on Experimental Gel Points during ATRcP of Monomer and Cross-Linker. *Macromolecules* **2008,** 41, 7843-7849.
14. Lindemann, B.; Schröder, U. P.; Oppermann, W. Influence of the Cross-Linker Reactivity on the Formation of Inhomogeneities in Hydrogels. *Macromolecules* **1997,** 30, 4073-4077.
15. Fan, H. L.; Wang, J. H.; Tao, Z.; Huang, J. C.; Rao, P.; Kurokawa, T.; Gong, J. P. Adjacent cationic–aromatic sequences yield strong electrostatic adhesion of hydrogels in seawater. *Nat. Commun.* **2019,** 10, 5127.
16. Mayo, F. R.; Lewis, F. M. Copolymerization. I. A Basis for Comparing the Behavior of Monomers in Copolymerization; The Copolymerization of Styrene and Methyl Methacrylate. *J. Am. Chem. Soc.* **1944,** 66, 1594-1601.
17. Matsukata, M.; Hirata, M.; Gong, J. P.; Osada, Y.; Sakurai, Y.; Okano, T. Two-step surfactant binding of solvated and cross-linked poly(N-isopropylacrylamide-co- (2-acrylamido-2-methyl propane sulfonic acid)). *Colloid. Polym. Sci.* **1998,** 276, 11-18.
18. Thévenot, C.; Khoukh, A.; Reynaud, S.; Desbrières, J.; Grassl, B. Kinetic aspects, rheological properties and mechanoelectrical effects of hydrogels composed of polyacrylamide and polystyrene nanoparticles. *Soft Matter* **2007,** 3, 437-447.
19. Mortimer, R. Physical Chemistry, 3rd Edition. *Academic Press, USA,* **2008**.
20. Fan, H. L.; Guo, H. L.; Wang, J. H.; Gong, J. P. Competitive cation−π interactions between small cations and polycations with phenyl groups in poly(cation−π) hydrogels. *Giant* **2020,** 1, 100005.
21. Chen, L.; Sun, T. L.; Cui, K.; King, D. R.; Kurokawa, T.; Saruwatari, Y.; Gong, J. P. Facile synthesis of novel elastomers with tunable dynamics for toughness, self-healing and adhesion. *J. Mater. Chem. A* **2019,** 7, 17334-17344.
22. Fan, H. L.; Wang, J. H.; Gong, J. P. Barnacle Cement Proteins-Inspired Tough Hydrogels with Robust, Long-Lasting, and Repeatable Underwater Adhesion. *Adv. Funct. Mater.* **2020**, 2009334.